Genome-wide Identification of the Laccase Gene Family in White Jute (*Corchorus capsularis*): Potential Targets for Lignin Engineering in Bast Fiber

Subhadarshini Parida[1†], Deepak Kumar Jha[1, 2†], Khushbu Kumari[1, 2], Seema Pradhan[1], Nrisingha Dey[1], Shuvobrata Majumder[1]*

[1] BRIC-Institute of Life Sciences (ILS), Department of Plant & Microbial Biotechnology, NALCO Square, Bhubaneswar, Odisha, PIN 751023, India.

[2] BRIC-Regional Centre for Biotechnology, Faridabad 121001, India.

*Corresponding author and email: shuvo@ils.res.in

[†] Equality contributed

Abstract:

Jute (*Corchorus* spp.) is an important industrial bast fibre crop valued for its lignocellulosic fibres, yet the molecular basis of fibre lignification remains unexplored. Laccase (EC 1.10.3.2) is a key enzyme catalysing the final steps of lignin polymerisation. A genome-wide analysis of white jute (*Corchorus capsularis*) identified 34 putative laccase genes (*CcaLAC*s), phylogenetically grouped into six clades. Expression profiling revealed predominant expression in phloem tissue (17 genes), followed by leaf (9) and xylem/root tissues (4). Several *CcaLAC*s showed progressive upregulation from early growth to harvest stages. Homology with *Arabidopsis* laccases highlighted candidate genes involved in lignification, which were further supported by transcriptomic and qRT-PCR analyses. Notably, key *CcaLAC*s showed significantly reduced expression in *dlpf*, a low-lignin white jute mutant. *CcaLAC* expression was also responsive to abiotic stresses, including abscisic acid and copper. MicroRNA target prediction identified Ath-miR397a and Ath-miR397b as potential regulators of multiple *CcaLAC*s. Structural and subcellular analyses revealed conserved motifs, transmembrane domains, and diverse cellular localization. Gene ontology analysis linked *CcaLAC*s to lignin and phenylpropanoid biosynthesis. Among them, *CcaLAC28* and *CcaLAC32* emerged as strong candidates regulating phloem fibre lignification, providing promising targets for developing low-lignin jute varieties for industrial applications.

Keywords: Jute; Laccase; Whole Genome Search; microRNA; Abiotic stress; Lignin pathway

1. Introduction:

Laccases (LACs) are multicopper oxidases widely present in plants, fungi, and bacteria. In plants, they catalyse the oxidation of phenolic substrates during lignin polymerisation, reducing molecular oxygen to water (**Berthet et al., 2012**). Their involvement in secondary cell wall formation and lignification has been demonstrated in tree species such as loblolly pine (*Pinus taeda*) and sycamore maple (*Acer pseudoplatanus*), as well as in model plant systems. However, the *LAC* gene family remains largely unexplored in jute (*Corchorus* spp.), a major lignocellulosic fibre crop.

Jute bast fibres are strong, biodegradable and widely used in packaging, textiles, paper and composite applications. Their comparatively high lignin content (12–26%) contributes to fibre coarseness and limits value-added applications relative to low-lignin flax (~2%) and lignin-free cotton (**Majumder et al., 2020a**). Improving fibre quality therefore requires a better understanding of lignification and its regulatory genes.

The reference genomes of white jute (*Corchorus capsularis*) and tossa jute (*C. olitorius*) have enabled genome-wide identification of lignin-related gene families (**Zhang et al., 2021**). For example, six *CCoAOMT* genes were identified as contributors to lignification in jute. Laccases (*LAC*) and peroxidases (*PRX*) jointly catalyse monolignol polymerisation during secondary cell wall formation, yet *LAC* genes have received less attention in jute compared to *PRX* genes.

Genome-wide surveys report medium-to-large *LAC* gene families across plant lineages, including 17 putative *LAC* genes in *Arabidopsis thaliana*, 30 in rice (*Oryza sativa*), 49 in black cottonwood (*Populus trichocarpa*), 54 in flooded gum (*Eucalyptus grandis*), 45 in flax (*Linum usitatissimum*), 84 in cotton (*Gossypium hirsutum*), 22 in maize (*Zea mays*), 156 in wheat (*Triticum aestivum*) and 46 in tossa jute (*Corchorus olitorius*) (**Jha et al., 2025**). Functional studies showed that *AtLAC4* and *AtLAC17* are essential for lignification in *Arabidopsis* stems (**Berthet et al., 2011**), and overexpression of *GaLAC1* increased lignification in poplar (**Wang et al., 2008**). In jute, a reduced-lignin mutant (*dlpf*) exhibits downregulation of phenylpropanoid

pathway genes, suggesting a regulatory role for laccases in bast fibre lignification (**Chakraborty et al., 2015**).

Laccases also participate in stress responses, such as desiccation, freezing, and high salinity in plants, often through ABA-mediated signalling linked to lignin deposition (**Vishwakarma et al., 2017**). However, stress-induced *LAC* gene expression has not been examined in jute. The *in-silico* study of upstream cis-acting elements of genes provides insights into the stress conditions or signaling pathways that regulate their expression. The presence of stress-, hormone- and development-related cis-elements may therefore provide functional clues.

The objective of this study is to identify and characterise the *LAC* gene family in white jute (*C. capsularis*), and to analyse their expression across tissues, developmental stages, and under copper stress and ABA treatment, to infer their potential roles in fibre lignification and stress adaptation.

These analyses will help prioritise candidate *CcaLAC* genes for future functional validation and molecular breeding to improve jute fibre quality.

2. Materials and Methods

2.1. Identification of Laccase Genes in White Jute and Sequence Analysis

The white jute genomic DNA, coding sequences (CDS), and protein sequences were retrieved from the Genome Warehouse (accession: GWHBCLC00000000; accessed November 28, 2023) following **Zhang et al. (2021)**.

Laccase (LAC) protein sequences from *O. sativa* (Oryzabase), *Arabidopsis thaliana* (TAIR), and *Theobroma cacao* (Phytozome) were used as references. A total of 74 LAC sequences were employed to construct a Hidden Markov Model (HMM) using HMMER v3.2, which was queried against the jute protein dataset to identify putative *C. capsularis* laccase (*CcaLAC*) genes.

Candidate sequences were validated for conserved laccase domains (PF07731.11, PF00394.19, PF07732.12) using NCBI CDD, HMM Scan, and SMART. Redundant hits (cut-off >0.01) were removed to retain non-redundant sequences. Physicochemical properties were predicted using ExPASy ProtParam, and transmembrane regions were analyzed using TMHMM v2.0.

2.2. Chromosome Mapping, Phylogenetic and Motif Analysis

Chromosomal locations of *CcaLAC* genes were visualized using MapInspect v1.0 based on their genomic coordinates (accessed November 28, 2023). Phylogenetic analysis was performed using laccase protein sequences from *C. capsularis*, *O. sativa*, *A. thaliana*, and *T. cacao*. *Arabidopsis* was included as a model dicot, rice as a representative monocot, and cacao due to its close genomic similarity with jute (**Zhang et al., 2021**). Multiple sequence alignment was carried out using MUSCLE, and phylogenetic trees were constructed in MEGA v10.0 using the maximum likelihood method with 1000 bootstrap replications, gap deletion, and a site-gamma (G) distribution model. Conserved motifs in CcaLAC proteins were identified using the MEME suite, with parameters set to a maximum of 10 motifs, minimum motif width of 6, and maximum width of 50 (**Chanwala et al., 2023**).

2.3. Gene Structure, Duplication, and Synteny Analysis

The exon–intron organization of *CcaLAC* genes was analyzed using the Gene Structure Display Server (GSDS). Gene duplication and mutation events within the *CcaLAC* family were investigated through BLASTp analysis against laccase proteins from *A. thaliana*, *O. sativa*, *T. cacao*, and *C. capsularis*, using e-value cutoff 0.01. Gene duplication events were defined based on ≥80% sequence similarity. To assess evolutionary divergence, synonymous (Ks) and nonsynonymous (Ka) substitution rates were calculated using the PAL2NAL program. Syntenic relationships among laccase genes were identified and visualized using TBtools.

2.4. Protein–Protein Interaction and Structural Prediction

Protein–protein interaction (PPI) networks for the candidate laccase proteins CcaLAC28 and CcaLAC32 were predicted using the STRING database (accessed April 2, 2025). Their *A. thaliana* orthologs, AtLAC4 and AtLAC17, respectively, were used as references for interaction inference. Secondary and tertiary structures of CcaLAC28 and CcaLAC32 were predicted using the Phyre2 server (accessed April 1, 2025). The predicted three-dimensional models were visualized and analyzed using ChimeraX software.

2.5. Cis-Element and microRNA Target Analysis

Upstream promoter regions (~2000 bp) of *CcaLAC* genes were retrieved from the *C. capsularis* genome for cis-regulatory element analysis. Putative cis-elements were identified using the PlantCARE database, with emphasis on elements associated with biotic and abiotic stress responses, growth and development, cell wall biosynthesis, circadian regulation, metabolism, and hormone signaling.

Arabidopsis mature microRNA (miRNA) sequences were obtained from the PmiREN2.0 database. Target sites of these miRNAs on *CcaLAC* genes were predicted using the psRNATarget server.

2.6. Gene Ontology Annotation

Gene Ontology (GO) annotation was performed to infer the functional roles of the *CcaLAC* gene family. *CcaLAC* protein sequences were searched against the UniProt-SwissProt database using BLASTp to identify homologs. The corresponding UniProt IDs were submitted to the Gene Ontology database (accessed January 15, 2025) for GO term assignment, with *A. thaliana* laccase proteins used as reference annotations.

2.7. Plant Material and Abiotic Stress Treatments

Seeds of *C. capsularis* variety JRC321, its low-lignin *dlpf* mutant (characterized by ~50% reduced lignin and superior fibre quality), and the corresponding control variety JRC212 were obtained from the Central Research Institute for Jute and Allied Fibres (CRIJAF), India. Plants were grown under greenhouse conditions (30 ± 2 °C, ~80% relative humidity, and a 13 h light/11 h dark photoperiod).

To examine tissue-specific expression of *CcaLAC* genes, leaf, root, xylem, and phloem tissues were collected from JRC321 plants at 60 days after sowing (DAS). For developmental stage–specific expression analysis, phloem tissues from JRC212 and *dlpf* plants were harvested at 30, 60, 90, and 120 DAS.

Abiotic stress treatments were performed on 60-day-old JRC321 plants. Abscisic acid (ABA; 0.15 mM) and copper stress (0.10 mM $CuSO_4 \cdot H_2O$) were applied following **Parida et al. (2024)**. Stem tissues were collected at 0, 2, 4, 8, 12, and 24 h post-treatment, using three biological replicates per time point. All samples were immediately frozen in liquid nitrogen and stored at −80 °C for RNA isolation.

2.8. *In-Silico* Analysis of *CcaLAC* Gene Expression

RNA-seq short reads derived from bast (phloem) tissues of control JRC212 and *dlpf* mutant genotypes were retrieved from the NCBI Sequence Read Archive (accession numbers SRR1585372 and SRR1585373, respectively). Reads were mapped against the coding sequences (CDS) of the 34 identified *CcaLAC* genes.

Transcript abundance was estimated using the Trinity RNA-seq pipeline scripts *align_and_estimate_abundance.pl* and *abundance_estimates_to_matrix.pl* (accessed July 10, 2024). TMM-normalized read counts were $\log_2$-transformed, and expression heatmaps were generated using MeV software (retrieved July 10, 2024).

2.9. Gene Expression Analysis by qRT-PCR

Total RNA was isolated from leaf, xylem, phloem, and root tissues of jute plants using a commercial RNA isolation kit (Macherey-Nagel, Germany). Approximately 100 mg of tissue was ground in liquid nitrogen, and RNA extraction was performed according to the manufacturer's protocol, including on-column DNase treatment to remove genomic DNA contamination. RNA integrity was verified on a 2% agarose gel, and concentration and purity were measured using a NanoDrop 2000c spectrophotometer (Thermo Scientific, USA).

First-strand cDNA was synthesized from 1 µg of total RNA using a first-strand cDNA synthesis kit (Thermo Scientific, USA). Gene-specific primers were designed using PrimerQuest (Integrated DNA Technologies, USA) with default parameters (Tm 59–62 °C, GC content 35–65%, primer length 17–30 bp, and amplicon size 75–150 bp). Primer sequences are listed in **Supplementary Table 1**.

qRT-PCR was performed using a QuantStudio™ 5 Real-Time PCR system (Thermo Scientific, USA). The cDNA was diluted 1:9 prior to amplification. PCR conditions included an initial denaturation at 95 °C for 2 min, followed by 40 cycles of 95 °C for 15 s, primer-specific annealing for 1 min, and extension at 95 °C for 15 s. Melt curve analysis was conducted from 60 °C to 95 °C to confirm amplification specificity. Jute ubiquitin-1 (*UBI*; GenBank accession GH985256) was used as the internal reference gene (**Parida et al., 2024**). Relative gene expression was calculated using the $2^{-\Delta\Delta Ct}$ method (**Livak and Schmittgen, 2001**). Three biological replicates were analyzed, each with three technical replicates.

Eight lignification-related Arabidopsis laccase genes (*AtLAC2, AtLAC4, AtLAC5, AtLAC10, AtLAC11, AtLAC12, AtLAC15,* and *AtLAC17*) were selected based on previous reports (**Berthet et al., 2012**). Homologous *CcaLAC* genes were identified through BLAST analysis using TBtools, and genes showing >60% sequence identity were selected for expression analysis (**Jha et al., 2024**). Expression of these homologous *CcaLAC* genes was evaluated in phloem and xylem tissues at 30, 60, 90, and 120 DAS to assess their role in lignification during jute development.

2.10. Statistical Analysis

A comprehensive analysis was done that included calculation of the mean Ct values using Microsoft Excel and performing a one-way ANOVA. In addition, the GraphPad Prism statistical software (version 9.0) was used to perform Tukey's multiple comparisons test.

3. Results

3.1. Gene Number, Structure, and Duplication Events in White Jute *Laccase* Genes (*CcaLACs*)

A total of 34 *laccase* genes were found, unevenly distributed across the seven chromosomes of white jute and designated *CcaLAC1* to *CcaLAC34* based on their chromosomal locations (**Figure** 1A). Chromosome 7 contained the highest number of *CcaLAC* genes (10 genes; *CcaLAC25–CcaLAC34*), followed by chromosome 1 with seven genes (*CcaLAC1–CcaLAC7*) and chromosome 2 with six genes (*CcaLAC8–CcaLAC13*). Chromosomes 4, 5, and 6 each harbored three *CcaLAC* genes, whereas chromosome 3 contained only two.

Substantial variation was observed in gene structure, with exon numbers ranging from 2 to 28 among the *CcaLAC* genes. *CcaLAC19* possessed the minimum number of exons (two), while *CcaLAC26* exhibited the most complex structure with 28 exons (**Figure** 1B).

Gene duplication analysis identified 20 paralogous *CcaLAC* gene pairs, including four tandem duplication events and sixteen segmental duplication events (**Supplementary Table 2**). In addition, 96 orthologous gene pairs were detected across species comparisons, comprising 21 pairs between *C. capsularis* and *O. sativa*, 21 pairs between *C. capsularis* and *A. thaliana*, and 54 pairs between *C. capsularis* and *T. cacao* (**Figure** 1C). The higher number of orthologous pairs between jute and cacao likely reflects their greater genomic similarity, as previously reported (**Zhang et al., 2021**).

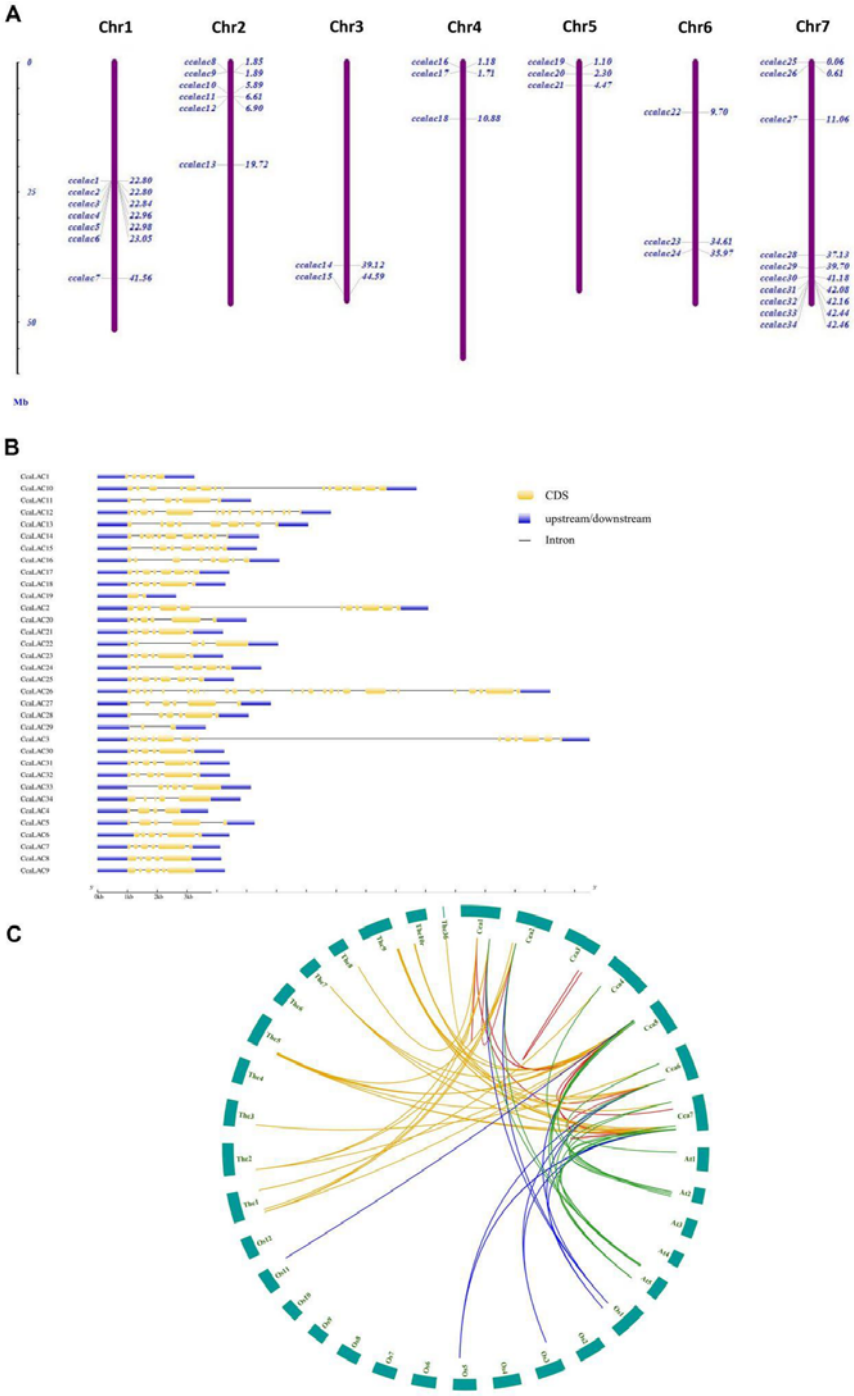

Figure 1. Number and gene structure of white jute (*C. capsularis*) laccase genes (*CcaLAC*s) (A) Chromosomal mapping of 34 laccase (*CcaLAC*) members in the genome. (B) Gene structure of CcaLACs. (C) Synteny relationship between white jute (*C. capsularis*), Arabidopsis (*A. thaliana*), rice (*O. sativa*), and cacao beans (*T. cacao*) *LAC* genes. Each coloured line represents duplicated gene pairs indicating the shared ancestry among the species.

3.2. Motif Analysis and Phylogenetic Relationships of Laccase Proteins in White Jute

The CcaLAC proteins exhibited considerable variation in size and physicochemical properties. Their molecular weights ranged from 11.65 kDa (CcaLAC29) to 177.31 kDa (CcaLAC26), with an average length of approximately 610 amino acids. The longest protein, CcaLAC26, consisted of 1,583 amino acids, whereas CcaLAC29 was the shortest, comprising 102 amino acids (**Table 1**). Most CcaLAC proteins displayed predicted instability indices below 40, indicating structural stability, except CcaLAC19 (41.63) and CcaLAC26 (43.34) (**Supplementary Table 3**). The aliphatic index ranged from 65.10 (CcaLAC29) to 93.14 (CcaLAC26), reflecting variability in thermal stability. All CcaLAC proteins showed negative average hydropathy values (<0), suggesting a predominantly hydrophilic nature. Subcellular localization analysis predicted that CcaLAC proteins are distributed across multiple cellular compartments (**Supplementary Table 3**). Notably, 18 of the 34 CcaLAC proteins (52.94%) were predicted to possess transmembrane domains (**Supplementary Figure 1**).

Motif analysis identified ten conserved motifs (motif-1 to motif-10) across the CcaLAC protein family (**Figure** 2A). Most motifs were conserved in the majority of CcaLAC proteins, although motif-3 and motif-6 were absent in several members. CcaLAC19 and CcaLAC29 contained only motif-3 and motif-1, respectively. Repetitions of specific motifs were observed in CcaLAC2, CcaLAC3, and CcaLAC10, suggesting possible functional diversification.

Phylogenetic analysis grouped the 34 CcaLAC proteins into six distinct clades (Groups I–VI) (**Figure** 2B). Group IV contained the largest number of members (16 proteins), followed by Group I (9 proteins) and Group III (7 proteins), while Groups II and V each contained a single protein. Functionally characterized Arabidopsis laccases clustered with their putative jute orthologs: AtLAC4, a key enzyme in lignification, grouped with CcaLAC28 in Group IV, whereas AtLAC17 clustered with its jute homolog CcaLAC32 in Group III (**Figure** 2B).

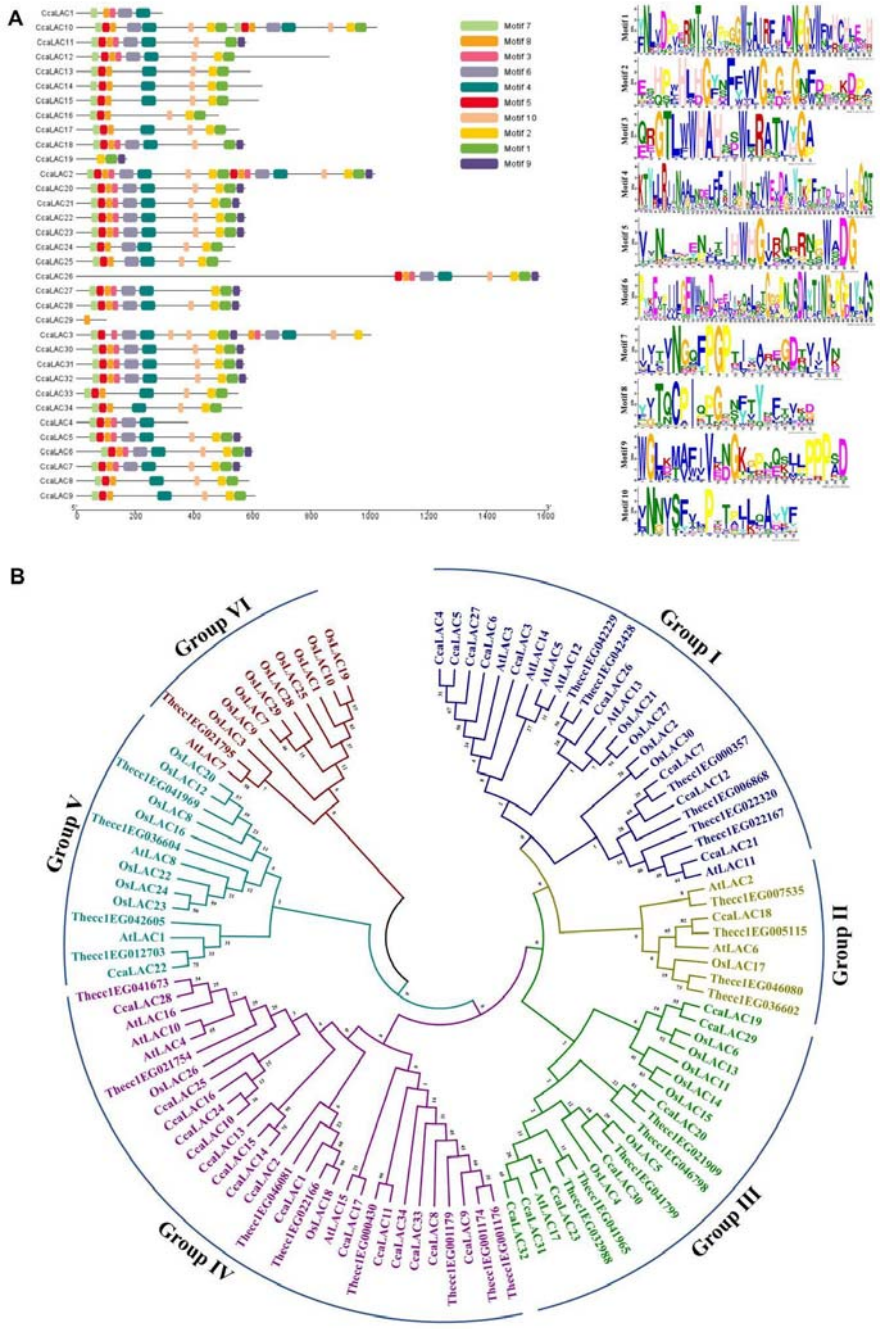

Figure 2. Conserved motif and phylogenetic analysis of CcaLAC proteins. (A) Conserved motif distribution in identified CcaLAC proteins. Motifs are indicated by different colours and their respective sequences. (B) Phylogenetic tree of LAC proteins of white jute (*C. capsularis*), rice (*Oryza sativa*), *A. thaliana*, and *T. cacao*. The analysis classified the LAC protein family members into six distinct groups. Abbreviations such as At (*Arabidopsis*), Os (rice), Thecc (*cacao*), and Cca (white jute) are used to denote laccase genes specific to each species.

Table 1. Bioinformatics Analysis and Physicochemical Properties of C*caLAC*s

Gene Name	Gene ID	Gene Length (bp)	Position	Amino Acid (aa)	pI	MW (kDa)	Subcellular Localization
CcaLAC1	GWHPBCLC001173	1330	Chr1	293	5.01	31.85	Chloroplast
CcaLAC2	GWHPBCLC001174	9172	Chr1	1020	6.03	113.52	Chloroplast
CcaLAC3	GWHPBCLC001176	14584	Chr1	1007	5.07	111.63	Endoplasmic Reticulum
CcaLAC4	GWHPBCLC001178	1789	Chr1	381	8.18	42.81	Cytoplasm
CcaLAC5	GWHPBCLC001179	3342	Chr1	566	7.31	63.59	Chloroplast
CcaLAC6	GWHPBCLC001182	2425	Chr1	603	8.64	67.82	Chloroplast
CcaLAC7	GWHPBCLC002591	2192	Chr1	563	8.45	62.29	Cytoplasm
CcaLAC8	GWHPBCLC003786	2149	Chr2	588	8.69	66.19	Mitochondria
CcaLAC9	GWHPBCLC003791	2275	Chr2	611	6.55	68.30	Cytoplasm
CcaLAC10	GWHPBCLC004194	8705	Chr2	1027	9.54	114.71	Cytoplasm
CcaLAC11	GWHPBCLC004256	3145	Chr2	580	7.27	64.94	Vacuoles
CcaLAC12	GWHPBCLC004295	5830	Chr2	862	8.85	95.54	Cytoplasm; Nucleus
CcaLAC13	GWHPBCLC005147	5065	Chr2	594	6.07	66.39	Vacuoles
CcaLAC14	GWHPBCLC008300	3416	Chr3	635	8.72	71.13	Golgi apparatus; Plasma Membrane
CcaLAC15	GWHPBCLC008874	3344	Chr3	622	6.92	69.90	Extracellular Space
CcaLAC16	GWHPBCLC009134	4102	Chr4	485	9.04	54.01	Golgi Apparatus
CcaLAC17	GWHPBCLC009197	2419	Chr4	555	9.12	62.23	Golgi Apparatus
CcaLAC18	GWHPBCLC010239	2289	Chr4	575	8.39	63.76	Extracellular Space
CcaLAC19	GWHPBCLC013380	635	Chr5	171	8.59	18.90	Nucleus
CcaLAC20	GWHPBCLC013482	2995	Chr5	576	9.3	63.87	Peroxisome
CcaLAC21	GWHPBCLC013679	2207	Chr5	561	9.37	62.58	Cytoplasm
CcaLAC22	GWHPBCLC016373	4059	Chr6	578	6.83	64.63	Cytoplasm
CcaLAC23	GWHPBCLC017617	2210	Chr6	577	8.86	63.68	Extracellular Space

CcaLAC24	GWHPBCLC017798	3491	Chr6	542	9.51	60.92	Endoplasmic Reticulum
CcaLAC25	GWHPBCLC018843	2576	Chr7	525	6.05	57.92	Chloroplast
CcaLAC26	GWHPBCLC018907	13184	Chr7	1583	6.66	177.31	Nucleus
CcaLAC27	GWHPBCLC019742	3813	Chr7	564	8.94	63.75	Chloroplast
CcaLAC28	GWHPBCLC020872	3070	Chr7	560	9.28	61.46	Vacuoles
CcaLAC29	GWHPBCLC021142	1626	Chr7	102	10.15	11.65	Nucleus
CcaLAC30	GWHPBCLC021267	2250	Chr7	576	9.41	63.62	Vacuoles
CcaLAC31	GWHPBCLC021382	2427	Chr7	574	9.19	63.11	Nucleus
CcaLAC32	GWHPBCLC021391	2443	Chr7	584	9.33	64.46	Nucleus
CcaLAC33	GWHPBCLC021419	3143	Chr7	551	6.36	61.84	Cytoskeletons
CcaLAC34	GWHPBCLC021420	2794	Chr7	565	6.4	63.17	Cytoplasm; Nucleus

3.3. Cis-acting Elements

A diverse array of cis-acting regulatory elements was identified in the upstream promoter regions of the 34 *CcaLAC* genes (**Supplementary Figure 2**). Core promoter elements such as MYB, MYC, and TATA-box motifs were present in all *CcaLAC* promoters. In addition, cis-elements associated with stress responsiveness (e.g., STRE, W-box, MYB, MYC, and WUN-motif), hormonal signalling (e.g., ABRE, ERE, P-box, GARE-motif, and TGA element), and tissue-specific and developmental regulation (e.g., G-box, GT1-motif, RY-element, Sp1, GATA-motif, LAMP element, Box-4, and TCT-motif) were abundant, suggesting functional diversification and complex regulatory control of *CcaLAC* gene expression (**Ain-Ali et al., 2021**; **Jha et al., 2024**).

Notably, several cis-elements implicated in secondary cell wall formation were detected upstream of multiple *CcaLAC* genes (**Supplementary Table 4**). These included AC elements (ACE), MYB binding sites (MBS), and G-box motifs, which are known to regulate lignin biosynthesis and secondary wall development, in addition to their roles in hormonal signalling (**Zhou et al., 2009**). The presence of these elements supports a potential involvement of *CcaLAC* genes in cell wall formation and lignification processes in white jute.

3.4. Tissue-Specific Expression Analysis of *CcaLAC* Genes

qRT-PCR analysis revealed detectable expression of all 34 *CcaLAC* genes across four tissues—phloem, xylem, leaf, and root. Transcript abundance was quantified as relative expression (RQ) values, with root tissue expression set as the reference (RQ = 1) (**Figure** 3).

Several *CcaLAC* genes exhibited higher expression in leaf tissue, including *CcaLAC3*, *CcaLAC12*, *CcaLAC17*, *CcaLAC22*, *CcaLAC23*, *CcaLAC27*, *CcaLAC29*, *CcaLAC32*, and *CcaLAC33*. Enhanced expression in phloem tissue was observed for *CcaLAC2*, *CcaLAC6*, *CcaLAC7*, *CcaLAC8*, *CcaLAC9*, *CcaLAC11*, *CcaLAC15*, *CcaLAC19*, *CcaLAC20*, *CcaLAC21*, *CcaLAC24*, *CcaLAC25*, *CcaLAC26*, *CcaLAC28*, *CcaLAC30*, *CcaLAC31*, and *CcaLAC34*. Higher transcript accumulation in xylem tissue was recorded for *CcaLAC4*, *CcaLAC5*, *CcaLAC16*, and *CcaLAC18*, whereas *CcaLAC1*, *CcaLAC10*, *CcaLAC13*, and *CcaLAC14* showed relatively higher expression in root tissue.

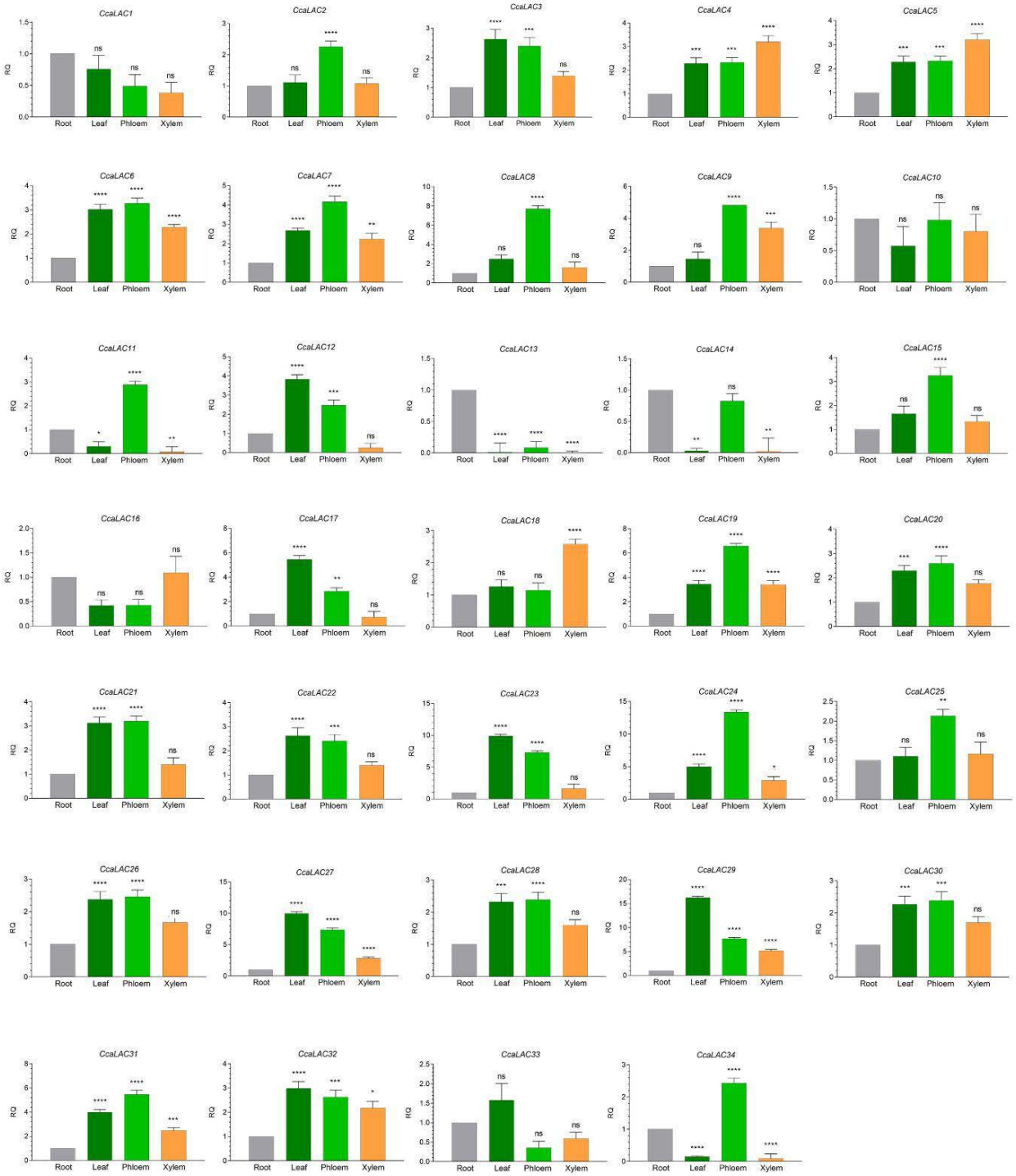

Figure 3. Tissue-specific expression of laccase (*CcaLAC*) genes. This figure shows the relative quantification (RQ) values of *CcaLAC* gene expression in the tissues of leaf, phloem, xylem, and root. The RQ values are normalised using the ubiquitin 1 (*UBI*) housekeeping gene. A one-way

ANOVA (*F*-test) with a significance threshold of $P \leq 0.05$, followed by Tukey's multiple comparisons test, was performed. Asterisks denote significant differences in *P* values from Tukey's test, while non-significant values are marked as 'ns'. The data represent three biological replicates.

3.5. Phloem Tissue-Specific Expression Analysis of *CcaLAC* Genes Across Developmental Stages

Expression profiling was performed at four key time points: 30 DAS, corresponding to the initiation of fibre development, and 60, 90, and 120 DAS, which represent progressive stages leading to fibre maturation and harvest. Several *CcaLAC* genes, including *CcaLAC19*, *CcaLAC21*, *CcaLAC23*, *CcaLAC28*, *CcaLAC29*, and *CcaLAC32*, exhibited a steady increase in transcript abundance from 30 DAS to 120 DAS (**Figure** 4). In contrast, *CcaLAC12*, *CcaLAC20*, *CcaLAC26*, and *CcaLAC30* showed a gradual increase in expression up to 90 DAS, followed by a marked decline at 120 DAS. Meanwhile, *CcaLAC7* and *CcaLAC31* displayed a slight reduction in expression at 120 DAS compared to earlier stages.

Overall, the majority of the analysed *AtLAC* homologous genes associated with the lignin biosynthetic pathway demonstrated increased expression in phloem tissue from 30 DAS to 90 DAS, coinciding with the active phase of fibre development and lignification.

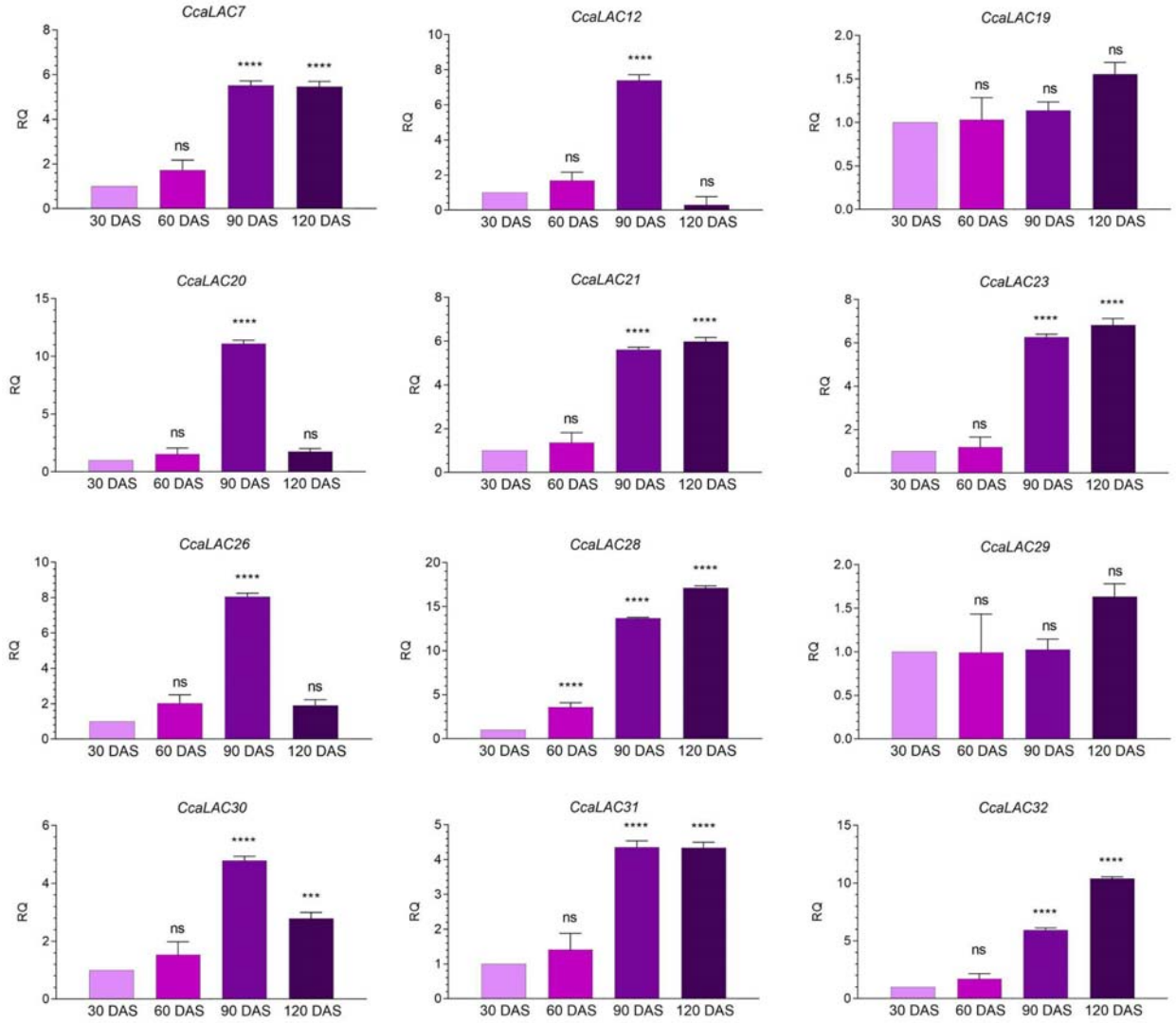

Figure 4. Expression of laccase (*CcaLAC*) genes at different developmental stages of white jute plants. This figure illustrates the expression of *CcaLAC*s in the phloem tissue of white jute at four different time points, from 30 to 120 days after sowing (DAS). A one-way ANOVA (*F*-test) with a significance threshold of $P \leq 0.05$, followed by Tukey's multiple comparisons test, was performed. Asterisks denote significant differences in *P* values from Tukey's test, while non-significant values are marked as 'ns'. The data represent three biological replicates.

3.6. Expression Analysis of *CcaLAC* Genes in the Low-Lignin Mutant Jute (*dlpf*)

In-silico expression analysis of *CcaLAC* genes was performed using RNA-seq data from 30 DAS phloem tissue of the white jute cultivar JRC212 and its X-ray-irradiated low-lignin mutant, *dlpf*, sourced from **Chakraborty et al. (2015)**. All 34 *CcaLAC* genes were expressed in phloem tissue (**Figure 5A**). Compared with JRC212, *dlpf* showed reduced expression of *CcaLAC3, CcaLAC4, CcaLAC7, CcaLAC9, CcaLAC17, CcaLAC18, CcaLAC21, CcaLAC23, CcaLAC31, CcaLAC32*, and *CcaLAC33*. To validate the RNA-seq results, nine *CcaLAC* genes were randomly selected for qRT-PCR analysis, which confirmed expression patterns consistent with the transcriptomic heatmap (**Supplementary Figure 3**).

Developmental expression analysis revealed that *CcaLAC21, CcaLAC23, CcaLAC28*, and *CcaLAC32*—genes that showed a progressive increase in expression from 30 to 120 DAS in JRC212—were significantly downregulated in *dlpf* at 90 and 120 DAS ($P < 0.0001$; **Figure** 5B). Similarly, *CcaLAC12, CcaLAC20,* and *CcaLAC26*, which exhibited peak expression at 90 DAS in JRC212, showed reduced expression in dlpf at the same stage. In contrast, *CcaLAC19* and *CcaLAC29* showed consistently low expression across all developmental stages in JRC212 and no significant differential expression in *dlpf* (**Supplementary Figure 4**).

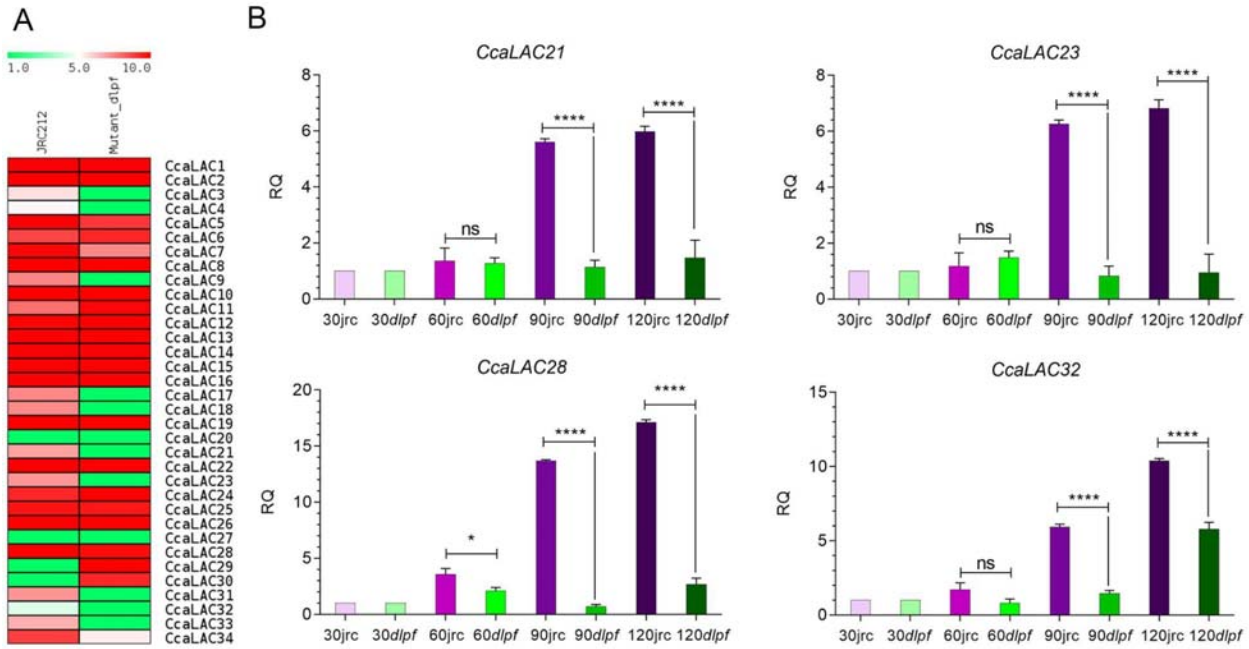

Figure 5. Expression analysis of white jute *laccase* genes in phloem tissue. (A) Expression analysis *in-silico* of *CcaLAC*s in the phloem tissue of JRC212 (control) and *dlpf* (mutant) at 30 DAS. Heat map is based on publicly available transcriptomics data from BioProject PRJNA255934. The expression scale ranges from low (1, green) to high (10, red). (B) This figure presents a comparative expression analysis of laccase (*CcaLAC*) genes of JRC212 and *dlpf* (which has fibres with 50% lower lignin content), across different developmental stages (30 DAYS to 120 DAS). A one-way ANOVA (F-test) with a significance threshold of $P \leq 0.05$, followed by Tukey's multiple comparisons test, was performed. Asterisks denote significant differences in *P* values from Tukey's test, while non-significant values are marked as 'ns'. The data represent three biological replicates.

3.7. Expression Analysis of *CcaLAC* Genes Under Copper Stress and ABA Treatment

CcaLAC28 and *CcaLAC32*, homologous to *A. thaliana AtLAC4* and *AtLAC17*, respectively, are among the highly expressed *CcaLAC* genes and are implicated in lignin biosynthesis. To evaluate their stress responsiveness, expression profiles were analysed under copper and abscisic acid (ABA) treatments.

Under copper stress, *CcaLAC28* showed a significant increase in expression at 12 h, whereas *CcaLAC32* exhibited significantly elevated expression at all examined time points (2–24 h). *CcaLAC32* expression increased gradually, peaked at 8 h, and subsequently declined (**Figure** 6A).

Under ABA treatment, both *CcaLAC28* and *CcaLAC32* showed significant induction at 8 h and 12 h, with maximum expression at 12 h followed by a decline at 24 h (**Figure** 6B). These expression patterns suggest that *CcaLAC28* and *CcaLAC32* function as delayed-responsive genes in white jute under ABA-mediated stress.

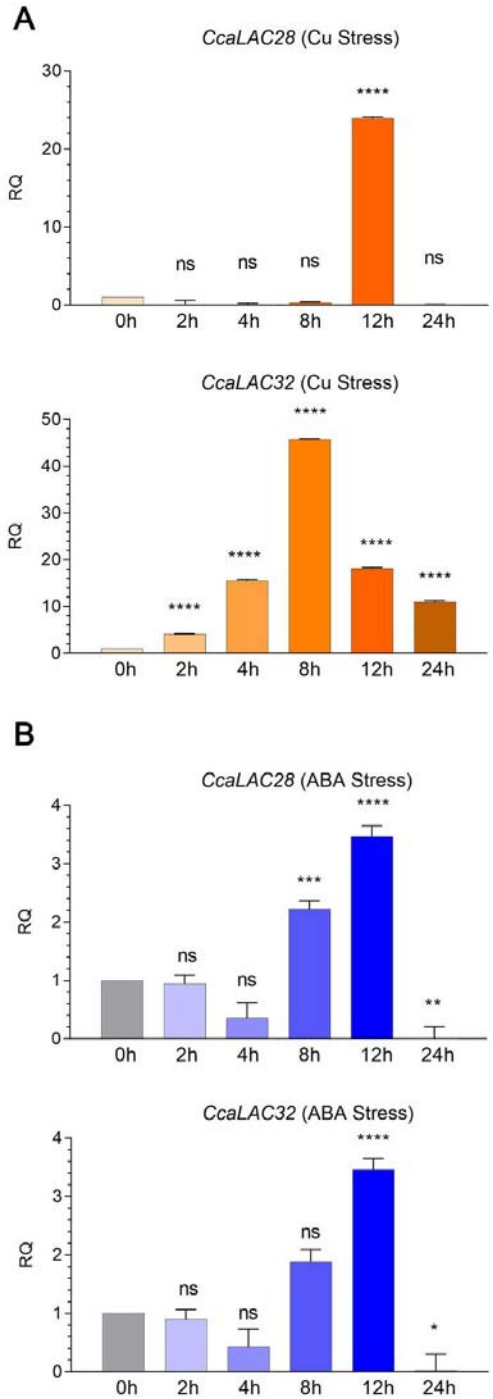

Figure 6. Expression of *CcaLAC28* and *CcaLAC32* under abiotic stresses. This figure depicts the *CcaLAC28* and *CcaLAC32* genes expression levels in (A) copper stress using (0.10 mM $CuSO_4 \cdot H_2O$), (B) ABA hormone stress. A one-way ANOVA (F-test) with a significance threshold of $P \leq 0.05$, followed by Tukey's multiple comparisons test, was performed. Asterisks

denote significant differences in *P* values from Tukey's test, while non-significant values are marked as 'ns'. The data represent three biological replicates.

3.8. Protein Structure Analysis of CcaLAC28 and CcaLAC32

The protein structures of CcaLAC28 and CcaLAC32 were predicted using Phyre2.2. CcaLAC28 (531 amino acids) was modeled with 100% confidence and showed 48% sequence identity with the crystal structure of *Z. mays* laccase 3 (ZmLAC3) complexed with sinapyl (fold library ID: c6kliA). The predicted secondary structure consisted of 39% β-strands, 4% α-helices, and 7% disordered regions, with a transmembrane domain predicted between residues 226 and 241 (**Figure** 7A). Similarly, CcaLAC32 (540 amino acids) was modeled with 100% confidence and exhibited 50% sequence identity with ZmLAC3. Its predicted secondary structure comprised 34% β-strands, 5% α-helices, and 4% disordered regions, with a transmembrane domain predicted between residues 136 and 151 (**Figure** 7B).

3.9. Protein–Protein Interaction Network Analysis

Protein–protein interaction networks were predicted *in-silico* using the STRING database. As the jute genome is not available in STRING, *Arabidopsis thaliana* (NCBI Taxonomy ID: 3702) was used as a reference to analyse the interaction networks of AtLAC4 and AtLAC17, homologous to CcaLAC28 and CcaLAC32, respectively.

CcaLAC28/AtLAC4 was predicted to interact with several enzymes and regulators associated with lignin biosynthesis and secondary cell wall formation, including phenylalanine ammonia-lyase (PAL1), cellulose synthase catalytic subunits (CESA4, CESA7, and CESA8), and transcription factors MYB63 and MYB46. Additional interactions were observed with proteins involved in secondary wall assembly, such as IRX9, IRX15, COBRA-like protein 4 (COBL4), and galacturonosyltransferase 1 (GAUT1) (**Figure** 7C).

Similarly, CcaLAC32/AtLAC17 was predicted to interact with PAL1, PAL2, PAL4, CESA4, CESA7, CESA8, and MYB63. In addition, unique interactions were identified with cinnamoyl-CoA reductase 1 (CCR1-2), CCR2-2, and chitinase-like protein 2 (CTL2), indicating a potential role in lignin biosynthesis, stress response, and cell wall organisation (**Figure** 7D).

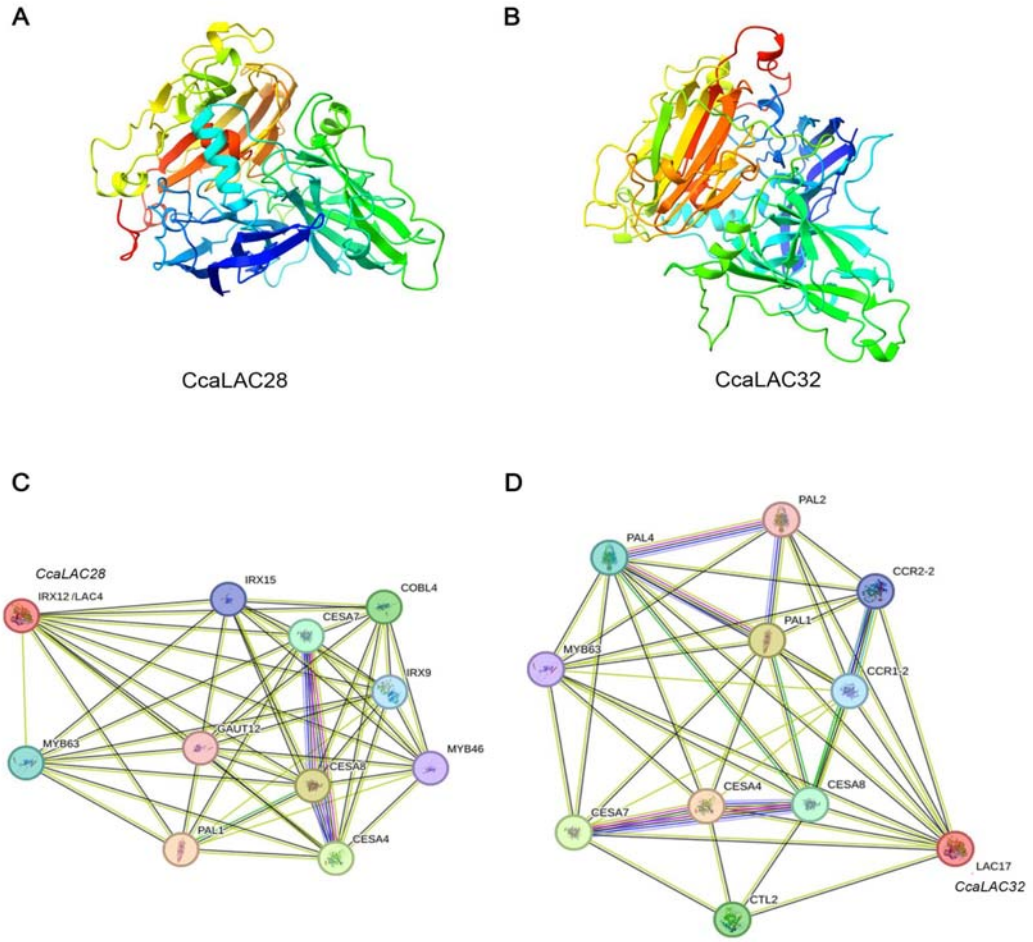

Figure 7. Predicted three-dimensional protein structures and Protein-protein interaction network analysis of CcaLAC28 and CcaLAC32. (A) The structural model of CcaLAC28 (531 amino acids) and (B) CcaLAC32 (540 amino acids) were generated using Phyre2.2. The structures are color-coded from the N-terminus (blue) to the C-terminus (red), highlighting secondary structural elements such as β-strands, α-helices, and loop regions. (C) Predicted interaction network of *CcaLAC28* (homologous to *AtLAC4*). (D) Predicted interaction network of

CcaLAC32 (homologous to *AtLAC17*). The STRING database used for protein-protein interaction network analysis.

3.10. MicroRNA (miRNA) Targeting of *CcaLAC* Genes

Several *CcaLAC* genes were predicted as targets of the lignin-associated miRNA miR397 (**Supplementary Table 5; Supplementary Figure 5**). Ath-miR397a was predicted to target *CcaLAC2, CcaLAC3, CcaLAC7, CcaLAC20, CcaLAC21, CcaLAC22, CcaLAC23, CcaLAC26, CcaLAC28, CcaLAC30,* and *CcaLAC31*, whereas Ath-miR397b targeted *CcaLAC7, CcaLAC20, CcaLAC21, CcaLAC22, CcaLAC23, CcaLAC28, CcaLAC30, CcaLAC31*, and *CcaLAC34*.

3.11. Functional Annotation of *CcaLAC* Genes by Gene Ontology (GO) Analysis

GO term analysis indicated that *CcaLAC* genes are primarily involved in lignin biosynthesis and metabolism, including lignin biosynthetic (GO:0009809), lignin metabolic (GO:0009808), phenylpropanoid biosynthetic (GO:0009699), and phenylpropanoid metabolic processes (GO:0009698) (**Supplementary Figure 6**). Additional enrichment was observed for secondary metabolite biosynthesis and metabolism. At the molecular function level, *CcaLACs* were associated with oxidoreductase activity, copper ion binding, and transition metal ion binding, consistent with the conserved biochemical roles of plant laccases (**Supplementary Figure 6**).

4. Discussion

The white jute genome contains 25,874 genes (**Zhang et al., 2021**), including the much unexplored laccase (*CcaLAC*) genes, especially regarding the function in stem development, fibre lignification, and performance under abiotic and biotic stress. The research was aimed at finding the functional importance of *LAC* in white jute (*C. capsularis*). The whole white jute genome was searched and 34 *CcaLAC* genes were identified; their expressions were examined in different tissues (**Figure 3**). Out of the 34 *CcaLAC* genes, 17 were highly expressed in phloem, 9 in leaves, 4 in xylem, and 4 in roots. Considering the stem part as a combination of phloem and

xylem tissue-specific expression, 61.76% of the *CcaLAC* genes are expressed here, which is highly significant in terms of the role of laccase in jute stem and fibre development. Such observations have been reported where *AtLAC* genes (*AtLAC2, AtLAC4, AtLAC10, AtLAC11, AtLAC16,* and *AtLAC17*), responsible for the lignification process, were expressed excessively in stem tissue of Arabidopsis (**Berthet et al., 2012**). This tissue-specific expression pattern of *LAC* genes in white jute (*C. capsularis*) differs from that observed in tossa jute (*C. olitorius*). In tossa jute, 43.47% (20 out of 46) of the *ColLAC* genes exhibited higher expression in roots compared to other tested tissues (**Jha et al., 2025**). This suggests potential differences in regulatory mechanisms between the two *Corchorus* species that govern the tissue-specific expression patterns of *LAC* genes.

Separation of xylem and phloem tissue from the jute stem is difficult in the initial days of its growth, but by 30 DAS it becomes much easier, suggesting that fibre development and the lignification process begin around this time (**Chakraborty et al., 2015**). By 110-120 DAS, phloem fibre can be easily extracted through the biological retting process, indicating its maturity and the completion of the lignification process. This research included targeting monthly time points of 30 DAS (one month), 60 DAS (two months), 90 DAS (three months), and finally 120 DAS (4 months) to relate *CcaLAC* expression with jute stem development and fibre lignification process.

As a part of this investigation to find the functional importance of *CcaLAC* in the fibre lignification process of jute, homologous genes from *Arabidopsis* were selected. *Arabidopsis* is commonly used for lignin pathway analysis in plants due to its lignified stem tissue, short life span, and its classification as a dicotyledonous plant (**Vanholme et al., 2010**). There is a remarkable similarity between the sequences of *CcaLAC* and *AtLAC* genes and their expression patterns also match those of *Arabidopsis*, increasing with plant development (**Berthet et al., 2011**) (**Figure 4**).

Mutation of Arabidopsis *AtLAC4* (homologous to *CcaLAC28*) and *AtLAC17* (homologous to *CcaLAC32*) individually resulted in a 10% reduction in lignin content, and when both genes (*AtLAC4+AtLAC17*) were mutated, lignin content was reduced by 39% (**Berthet et al., 2011**). This same study on the double mutant line also demonstrated that *AtLAC4* and

AtLAC17 contributed significantly to total laccase enzyme activity in the plants, with about a 50% reduction in laccase activity observed upon their mutation. Recently, overexpression of *AtLAC4* in populus increased lignin content in the transgenic populus without any phenotypic changes in the plants (**Ahlawat et al., 2024**). These findings established the involvement of *AtLAC* in the lignification process, specifically *AtLAC4* and *AtLAC17*. This suggests that their homologous genes, *CcaLAC28* and *CcaLAC32*, might also have significant contribution in the process of lignification. The transcriptional expression of *CcaLAC* genes was tested at different developmental stages (30 DAS to 120 DAS) of jute plants through qRT-PCR estimation of mRNA transcripts. Four genes—*CcaLAC21, CcaLAC23, CcaLAC28,* and *CcaLAC32*—showed a steady increase in expression as the plant developed (**Figure 4**). This raised the question: Are these genes important in the process of lignin production in jute? Finding the answer led us to examine the expression of these four *CcaLAC* genes in a low lignin fibre content mutant variety of white jute, *dlpf* at various stages of growth. We found statistically significant differences upon comparing the expression patterns of these four *CcaLAC* genes of low-lignin mutant-*dlpf* with that of its control, JRC212. Lower expression patterns of *CcaLAC21, CcaLAC23, CcaLAC28* and *CcaLAC32* were found, which could be a contributing factor to the low lignin concentration observed in *dlpf* (**Figure 5B**). Although *dlpf* is an X-ray-irradiated mutant and may have mutations in other lignin pathway genes, the differential expression pattern of its control (JRC212) on four *CcaLAC* genes (*CcaLAC21, CcaLAC23, CcaLAC28,* and *CcaLAC32*) suggests that these genes are potential candidates for further investigation.

The expression of *CcaLAC12, CcaLAC20,* and *CcaLAC26* was significantly higher at 90 DAS, but decreased at 120 DAS to levels similar to those observed at 30 DAS (**Supplementary Figure 4**). If these genes were solely involved in the lignification process, their expression should remain high until 120 DAS (like *CcaLAC21, CcaLAC23, CcaLAC28* and *CcaLAC32*). The observed decrease in expression suggests their potential role in stem elongation or structure, which might be achieved by 90 DAS. Further functional characterization is necessary to confirm this hypothesis. This expression pattern was also observed in the *dlpf* mutant (**Supplementary Figure 4**).

Conversely, *CcaLAC19* and *CcaLAC29* maintained baseline expression levels throughout the developmental stages in both the control JRC212 and its mutant, *dlpf*, with no significant

changes (**Supplementary Figure 4**). This consistent expression suggests a fundamental role played by these genes in white jute development.

Previous studies (up to 60 DAS) on the low-lignin mutant jute, *dlpf*, by **Chakraborty et al. (2015)** found a low expression of cinnamyl alcohol dehydrogenase (CAD), considered to be essential the lignin pathway. This recent study on the *dlpf* (plants up to 120 DAS) lignin pathway involved comparing the qRT-PCR expression data using two housekeeping genes- *UBI* and *beta-tubulin* (*BTUB*) (**Parida et al., 2024)**. We found the expression of *CCoAoMT*, cinnamate 4-hydroxylase (*C4H*), and *CAD* to be lower in *dlpf* than in its control JRC212. This study represents the first analysis of *LAC* gene expression in the low-lignin mutant *dlpf*. Although transcriptomic data (BioProject PRJNA255934) from **Chakraborty et al. (2015)** reported 15 unigenes annotated as *LAC* genes in *JRC212* and *dlpf*, no qRT-PCR-based expression analysis was conducted. Here, we utilized the same transcriptomic dataset to examine the *in-silico* expression profiles of all 34 *CcaLAC* genes, revealing distinct expression patterns (**Figure 5A**). The low expression levels of *CcaLAC21*, *CcaLAC23*, *CcaLAC28* and *CcaLAC32* in *dlpf* may also contribute to the reduced lignin content, but further functional validation of these *CcaLAC* genes is needed (**Figure 5B**).

The expression pattern of plant laccases is influenced by transcriptional and post-transcriptional factors. The MYB transcription factors regulate *LAC*, as reported in multiple plant studies. They are one of the largest transcription factor families that are most functionally diverse. In Arabidopsis, *AtMYB58* directly regulates *AtLAC4* expression; *AtMYB46* regulates *AtLAC10* and *AtHY5* regulates *AtLAC12* (**Zhou et al., 2009**). In bamboo (*Phyllostachys edulis*), *PeMYB4.1/20/85.2* regulates *PeLAC20*; in pear (*Pyrus bretschneideri*), *PbMYB26* regulates *PbLAC4*-like; and in Pearl millet (*Pennisetum glaucum*), *PgMYB305* regulates *PgLAC14* (**Bai et al., 2023**). A predominance of MYB binding sites were found in many jute laccases (*CcaLAC* genes) after analysis of cis-elements in their upstream sequences (**Supplementary Figure 2**). MYB were found upstream of *CcaLAC19*, *CcaLAC21*, *CcaLAC23*, *CcaLAC28*, *CcaLAC29*, and *CcaLAC32*, indicating that these genes could be regulated by MYBs. Recently, 88 MYBs were identified in white jute through a whole genome search, but it remains to be determined which MYBs regulate *CcaLAC* expression (**Niyitanga et al., 2023**).

The role of miRNAs in regulation of LAC has been reported in multiple plants, including rice, Arabidopsis, and Populus. MicroRNA397 (miR397) is directly targeting laccase transcripts and controlling their expression in plants. In Populus, miR397 targets 28 *PtLAC* genes (**Lu et al., 2013**). In chickpea (*Cicer arietinum*), miR397 targets *CaLAC4* and *CaLAC17* among the 20 identified *CaLAC* genes (**Sharma et al., 2023**). Similarly, miR397 plays a regulatory role in controlling *OsLAC* expression in rice (**Bakhshi et al., 2016**). It is considered as a negative regulator of *LAC* expression in lignin biosynthesis, as reported in rice, chickpea, Arabidopsis, and Populus. Are the jute *CcaLACs* targeted by miR397? We found that miR397a targets 11 *CcaLAC*s, and miR397b targets 9 *CcaLAC*s in white jute (**Supplementary Figure 5**). *CcaLAC28* (homologous to *AtLAC4*) is targeted by both miR397a and miR397b, but no target site was found on *CcaLAC32* (homologous to *AtLAC17*). Overexpression of miR397 in jute could provide more information on its involvement in the lignification process by regulating *CcaLACs* in the near future.

The assortment of cis-acting elements located in the upstream promoter regions of white jute *CcaLACs* suggests that the expression of *CcaLAC* genes may be influenced by diverse factors, including plant growth, developmental stages, hormonal signals, and both abiotic and biotic stresses (**Supplementary Figure 2**). Notably, cis-acting elements associated with secondary wall formation, such as AC elements (ACE), G-box motifs, and MYB Binding Sites (MBS), were identified in multiple *CcaLACs* (**Supplementary Table 4**). **Zhou et al. (2009)** demonstrated in *Arabidopsis* that *AtMYB58* and *AtMYB63* directly activate lignin biosynthetic genes by targeting ACE. **Zhao et al. (2010)** also reported that the lignin-specific transcription factor *AtMYB58* in *Arabidopsis* can directly activate most lignin biosynthetic genes through ACE binding in their promoters. Additionally, G-box motifs or G-box Regulating Factors (GRFs) are known to play crucial roles in plant physiological and developmental processes as well as in stress responses (**Sun et al., 2022**). The presence of these cis-acting elements in the *CcaLAC* members highlights their potential involvement in the lignification process and secondary wall formation in jute.

It is well-documented that laccase (*LAC*) genes are susceptible to environmental changes, with expression being up- or down-regulated by various abiotic factors (heavy metal ions, drought, salinity, temperature, oxidative stress) and biotic factors (pathogens, insects, fungi)

(reviewed by **Bai et al., 2023**), no studies have yet examined the expression patterns of jute LAC under stress conditions. The expression pattern of *CcaLAC28* (homologous to *AtLAC4*) and *CcaLAC32* (homologous to *AtLAC17*) genes was validated under two different stress conditions: ABA hormone and copper heavy metal stress.

Why were these (copper and ABA) specific abiotic stresses chosen? Copper is an essential heavy metal and a cofactor for laccase, playing a critical role in its catalytic function. The GO term assignment revealed that the *CcaLAC* genes are associated with the molecular function of copper ion binding (GO:0005507) (**Supplementary Figure 6**). This suggests that some of the identified 34 *CcaLAC* genes might respond to copper, a hypothesis that was further tested under 0.10 mM $CuSO_4 \cdot H_2O$ stress. Under copper stress, significant differences in *LAC* gene expression were observed, with *CcaLAC28* showing a 23.96-fold increase at 12 h and *CcaLAC32* showing a 45.73-fold increase at 8 h compared to the 0 h samples (**Figure 6A**). Such high expression was also previously recorded in rice laccase 10 (*OsLAC10*) under copper stress, which showed a 1200-fold increase at 12 h (**Liu et al., 2017**). Our goal was to identify *CcaLAC* genes involved in the lignification process, and copper stress was applied based on previous reports to identify responsive genes that could potentially be laccases. Further biochemical analysis will be required to confirm their laccase activity.

ABA hormone stress mimics conditions of multiple stresses like desiccation, freezing and high salinity in plants. Additionally, literature supports that drought stress can alter laccase expression in plants (**Sharma et al., 2023**). We found that *CcaLAC28* (homologous to *AtLAC4*) and *CcaLAC32* (homologous to *AtLAC17*) responded to ABA stress (**Figure 6B**). The presence of cis-acting elements such as MYC, MYB, CAT-box, and W-box which are known for ABA responsiveness in plants, likely explains this expression pattern (**Fujita et al., 2011**). These elements are also involved in drought and salinity stresses, suggesting that these genes might respond to those conditions as well. Further studies on *CcaLAC* gene expression and functionality, under the influence of various biotic and abiotic stresses, will provide more information on LAC's upstream cis-acting elements and their interactions with stress.

The expression of *CcaLAC*s in plant cells (subcellular localization) was predicted *in-silico* (**Supplementary Table 3**). Nucleus-specific localization was predicted for five *CcaLACs*

(*CcaLAC19, CcaLAC26, CcaLAC29, CcaLAC31,* and *CcaLAC32*), whereas nucleus and cytoplasm-specific localization were predicted for *CcaLAC12* and *CcaLAC34*. *In-silico* subcellular localization studies for *CcaLACs* provided vital information by predicting its location in cellular organelles, such as the chloroplast, plasma membrane, endoplasmic reticulum, mitochondria, Golgi apparatus, peroxisome, vacuoles, cytoskeletons, and extracellular spaces. The distribution of *CcaLACs* in cells was observed from the *in-silico* subcellular localization data. The presence of *CcaLACs* in all these membrane-bound compartments could be attributed to the presence of transmembrane helices in the majority (18 of 34) of *CcaLAC*s, as found in our analysis (**Supplementary Figure 1**). The structure of the plant laccase is still not well studied. Information about the presence of transmembrane helices could provide valuable insights into its structure.

Functional role analysis of *CcaLAC* genes through Gene Ontology (GO) term assignment identified 34 *CcaLAC* genes in white jute as being associated with key biological processes, including the phenylpropanoid biosynthetic (GO:0009699) and metabolic (GO:0009698) pathways (**Supplementary Figure 6**). Lignin, a crucial structural polymer in plants, is a product of the phenylpropanoid pathway. The GO term analysis further predicted that these *CcaLAC* genes are involved in the lignin biosynthetic (GO:0009809) and metabolic (GO:0009808) processes. While these functional roles are supported by the GO term assignment, experimental validation is required to confirm these predictions.

Manipulation of *LAC* genes has successfully altered lignin content in several crops. Downregulation of *GhLAC1* in cotton, *TaLAC4* in wheat, and overexpression of LACs in pear and silvergrass (*Miscanthus* sp.) significantly impacted lignin deposition (**Hu et al., 2020; Cheng et al., 2019; He et al., 2019**). In jute, targeted downregulation of lignin pathway genes has already been achieved, and phloem-specific silencing using the AtSUC2 promoter offers a strategy to reduce lignin without compromising plant fitness (**Majumder et al., 2020b**). Given their expression patterns and regulatory features, *CcaLAC28* and *CcaLAC32* emerge as promising targets for developing low-lignin jute varieties, warranting detailed functional validation.

5. Conclusion

The white jute (*C. capsularis*) genome harbours 34 putative laccase genes (*CcaLAC1–CcaLAC34*) distributed across its seven chromosomes. The expression of these genes was validated using publicly available transcriptomic datasets, revealing that a majority are preferentially expressed in phloem tissue. Gene Ontology (GO) annotation further supports their involvement in lignin biosynthesis and associated phenylpropanoid pathways. Among the identified laccases, *CcaLAC28* and *CcaLAC32* emerged as strong candidates for roles in stem lignification, based on their close sequence homology to well-characterised Arabidopsis lignin-associated laccases. Both genes exhibited a progressive increase in expression during plant development but showed significantly reduced expression in the low-lignin mutant *dlpf*, which contains approximately 50% less lignin than the control. Collectively, these findings provide a comprehensive foundation for understanding laccase-mediated lignification in white jute. Future functional validation of key *CcaLAC* genes, particularly *CcaLAC28* and *CcaLAC32*, may facilitate targeted modification of lignin content, thereby supporting the development of low-lignin jute fibres to meet growing industrial demands for sustainable and biodegradable fibre-based diversified products.

Funding

This research received funding from the Department of Biotechnology, Government of India, New Delhi, India under the project titled "Metabolic Engineering of Jute Stem for Lowering its Lignin Content and Improving its Fibre Quality" (project number BT/HRD/MKYRFP/50/17/2021, sanctioned on February 2, 2022).

Acknowledgments

We extend our sincere gratitude to the Director of the ICAR-Central Research Institute for Jute and Allied Fibres (CRIJAF), Kolkata, India, for providing the jute seeds. We also thank Prof. Swapan K. Datta and Dr. Karabi Datta from the Department of Botany, University of Calcutta,

Kolkata, India, for their valuable suggestions. We are deeply appreciative of the late Dr. Ajay Parida, former Director, and Dr. Debasis Dash, Director of ILS, Bhubaneswar, Odisha, India, for their unwavering support and essential facilities critical to the success of this project. We acknowledge Mrs. Soma Roy for her valuable comments and suggestions as an internal reviewer.

CRediT Authorship Contribution Statement

Subhadarshini Parida: Formal analysis, Investigation, Methodology, Writing – original draft. **Deepak Kumar Jha:** Formal analysis, Investigation, Methodology, Writing – original draft. **Khushbu Kumari:** Formal analysis, Investigation, Methodology, Writing – original draft. **Seema Pradhan:** Formal analysis, Data curation, Methodology, Writing– review & editing. **Nrisingha Dey:** Methodology, Writing - review & editing. **Shuvobrata Majumder:** Conceptualization, Investigation, Formal analysis, Funding acquisition, Methodology, Writing - review & editing.

Data availability

Data is provided within the manuscript or supplementary information files.

Conflict of Interest Statement

The authors declare no conflicts of interest.

Reference

Ahlawat, Y. K., Biswal, A. K., Harun, S., Hrman-Ware, A., Doeppke, C., Sharma, N., Joshi, C.P., & Hankoua B. B. (2024). Heterologous expression of Arabidopsis laccase2, laccase4 and peroxidase52 driven under developing xylem specific promoter DX15 improves saccharification in populus. *Biotechnology for Biofuels and Bioproducts* ,17, 5. https://doi.org/10.1186/s13068-023-02452-7

Ain-Ali, Q-u., Mushtaq, N., Amir, R., Gul, A., Tahir, M., & Munir, F. (2021). Genome-wide promoter analysis, homology modeling and protein interaction network of Dehydration Responsive Element Binding (DREB) gene family in *Solanum tuberosum*. *PLoS ONE*, 16 (12), e0261215. https://doi.org/10.1371/journal.pone.0261215

Bai, Y., Ali, S., Liu, S., Zhou, J., & Tang, Y. (2023). Characterization of plant laccase genes and their functions. *Gene*, 852, 147060. https://doi.org/10.1016/j.gene.2022.147060

Bakhshi, B., Mohseni Fard, E., Nikpay, N., Ebrahimi, M. A., Bihamta, M. R., Mardi, M., & Salekdeh, G. H. (2016). MicroRNA signatures of drought signaling in rice root. *PLoS One*, 11, e0156814. https://doi.org/10.1371/journal.pone.0156814

Berthet, S., Demont-Caulet, N., Pollet, B., Bidzinski, P., Cezard, L., Le Bris, P., Borrega, N., Herve, J., Blondet, E., Balzergue, S., Lapierre, C., & Jouanin, L. (2011). Disruption of *LACCASE4* and *17* results in tissue-specific alterations to lignification of *Arabidopsis thaliana* stems. *The Plant Cell*, 23, 1124–1137. https://doi.org/10.1105/tpc.110.082792

Berthet, S., Thevenin, J., Baratiny, D., Demont-Caulet, D., Debeaujon, I., Bidzinski, P., Leple, J-C., Huis, R., Hawkins, S., Gomez, L., Lapierre, C., & Jouanin, L. (2012). Role of plant laccases in lignin polymerization, Editor(s): Lise Jouanin, Catherine Lapierre, *Advances in Botanical Research*, Academic Press, 61, 145–172, https://doi.org/10.1016/B978-0-12-416023-1.00005-7

Chakraborty, A., Sarkar, D., Satya, P., Karmakar, P. G., & Singh, N.K. (2015). Pathways associated with lignin biosynthesis in lignomaniac jute fibres. *Molecular Genetics and Genomics*, 290 (4), 1523–1542. https://doi.org/10.1007/s00438-015-1013-y

Chanwala, J., Khadanga, B., Jha, D. K., Sandeep, I. S., & Dey, N. (2023). MYB transcription factor family in pearl millet: Genome-wide identification, evolutionary progression and expression analysis under abiotic stress and phytohormone treatments. *Plants*, 12, 355. https://doi.org/10.3390/plants12020355

Cheng, X., Li, G., Ma, C., Abdullah, M., Zhang, J., Zhao, H., Jin, Q., Cai, Y., & Lin, Y. (2019). Comprehensive genome-wide analysis of the pear (*Pyrus bretschneideri*) laccase gene (*PbLAC*) family and functional identification of *PbLAC1* involved in lignin biosynthesis. *PLoS One*, 14 (2), e0210892. https://doi.org/10.1371/journal.pone.0210892

Fujita, Y., Fujita, M., Shinozaki, K., & Yamaguchi-Shinozaki, K. (2011). ABA-mediated transcriptional regulation in response to osmotic stress in plants. *Journal of Plant Research*, 124, 509–525. https://doi.org/10.1007/s10265-011-0412-3

He, F., Machemer-Noonan, K., Golfier, P., Unda, F., Dechert, J., Zhang, W., Hoffmann, N., Samuels, L., Mansfield, S. D., Rausch, T., & Wolf, S. (2019). The *in vivo* impact of MsLAC1, a Miscanthus laccase isoform, on lignification and lignin composition contrasts with its *in vitro* substrate preference. *BMC Plant Biology*, 19 (1), 552. https://doi.org/10.1186/s12870-019-2174-3

Hu, Q., Xiao, S., Guan, Q., Tu, L., Sheng, F., Du, X., & Zhang, X. (2020). The laccase gene GhLac1 modulates fiber initiation and elongation by coordinating jasmonic acid and flavonoid metabolism. Crop J. 8 (4), 522–533. https://doi.org/10.1016/j.cj.2019.11.006

Jha, D.K., Chanwala, J., Barla, P., & Dey, N. (2024) Genome-wide identification of *bZIP* gene family in Pearl millet and transcriptional profiling under abiotic stress, phytohormonal treatments; and functional characterization of *PgbZIP9*. *Frontiers in Plant Science*, 15, 1352040. https://doi.org/10.3389/fpls.2024.1352040

Jha, D. K., Parida, S., Pradhan, S., Dey, N., & Majumder, S. (2025). Genome-wide analysis of the *laccase* gene family in tossa Jute (*Corchorus olitorius*): Insights into stem development, lignification, and responses to abiotic stress. *Frontiers in Plant Science*, 16, https://doi.org/10.3389/fpls.2025.1568674

Liu, Q., Luo, L., Wang, X., Shen, Z., & Zheng, L. (2017). Comprehensive analysis of rice laccase gene (*OsLAC*) family and ectopic expression of *OsLAC10* enhances tolerance to copper stress in *Arabidopsis*. *International Journal of Molecular Sciences*, 18 (2), 209. https://doi.org/10.3390/ijms18020209

Livak, K.J., & Schmittgen, T.D. (2001). Analysis of relative gene expression data using real time quantitative PCR and the $2^{-\Delta\Delta CT}$ method. *Methods*, 25, 402–408. https://doi.org/10.1006/meth.2001.1262

Lu, S., Li, Q., Wei, H., Chang, M.J., Tunlaya-Anukit, S., Kim, H., Liu, J., Song, J., Sun, Y-H., Yuan, L., Yeh, T-F., Peszlen, I., Ralph, J., Sederoff, R. R., & Chiang, V. L. (2013). Ptr-miR397a is a negative regulator of *laccase* genes affecting lignin content in *Populus trichocarpa*. *Proceedings of the National Academy of Sciences USA*, 110, 10848–10853. https://doi.org/10.1073/pnas.1308936110

Majumder, S., Datta, K., & Datta, S. K. (2024). Pyramided transgenic jute (*Corchorus capsularis*) with biotic stress resistance and herbicide tolerance. *Industrial Crops and Products*, 208. 117776. https://doi.org/10.1016/j.indcrop.2023.117776

Majumder, S., Saha, P., Datta, K., & Datta, S. K. (2020a). Fibre crop, jute improvement by using genomics and genetic engineering. In: Tuteja, N., Tuteja, R., Passricha, N., Saifi, S.K. (Eds.), *Advancement in Crop Improvement Techniques.* Woodhead Publishing with Elsevier Inc. Amsterdam, Netherlands, pp, 363–383. https://doi.org/10.1016/B978-0-12-818581-0.00022-X

Majumder, S., Datta, K., Satpathy, S., & Datta, S. K. (2020b). Development and evaluation of lepidopteran insect resistant jute expressing the fused *Bt*—Cry1Ab/Ac toxin driven by CaMV35S promoter. *Industrial Crops and Products*, 156, 112873. https://doi.org/10.1016/j.indcrop.2020.112873

Niyitanga, S., He, Q., Li, H., Ishimwe, C., Qi, J., Fang, P., Xu, J., Tao, A., & Zhang, L. (2023). Genome-wide identification and expression analysis of MYB transcription factors involved in fiber formation in white jute (*Corchorus capsularis*). *Industrial Crops and Products*, 197. 116539. https://doi.org/10.1016/j.indcrop.2023.116539

Parida, S., Datta, S. K., Dey, N., & Majumder, S. (2024). Selection of stable housekeeping genes for qPCR in biotic and abiotic stressed jute and their application in lignin pathway analysis, *Plant Stress*, 13, 100525. https://doi.org/10.1016/j.stress.2024.100525

Sharma, N.K., Yadav, S., Gupta, S.K., Irulappan, V., Francis, A., Senthil-Kumar, M., & Chattopadhyay, D. (2023). MicroRNA397 regulates tolerance to drought and fungal infection by regulating lignin deposition in chickpea root. *Plant Cell and Environment*, 46, 3501–3517. https://doi.org/10.1111/pce.14666

Sun, Q., Xi, Y., Lu, P., Lu, Y., Wang, Y., & Wang, Y. (2022). Genome-wide analysis of the G-box regulating factors protein family reveals its roles in response to *Sclerotinia sclerotiorum* infection in rapeseed (*Brassica napus* L.). *Frontiers in Plant Science*, 13:986635. https://doi.org/10.3389/fpls.2022.986635

Vanholme, R., Acker, R. V., & Boerjan, W. (2010). Potential of Arabidopsis systems biology to advance the biofuel field. *Trends in Biotechnology*, 28, 543–547. https://doi.org/10.1016/j.tibtech.2010.07.008

Vishwakarma, K., Upadhyay, N., Kumar, N., Yadav, G., Singh, J., Mishra, R. K., Kumar, V., Verma, R., Upadhyay, R. G., Pandey, M., & Sharma, S. (2017). Abscisic Acid Signaling and Abiotic Stress Tolerance in Plants: A Review on Current Knowledge and Future Prospects. *Frontiers in Plant Science*, 8:161. https://doi.org/10.3389/fpls.2017.00161

Wang, J., Wang, C. L., Zhu, M. L., Yu, Y., Zhang, Y., & Wei, Z. (2008). Generation and characterization of transgenic poplar plants overexpressing a cotton *laccase* gene. *Plant Cell, Tissue and Organ Culture*, 93, 303–310. https://doi.org/10.1007/s11240-008-9377-x

Zhang, L., Ma, X., Zhang, X., Xu, Y., Ibrahim, A. K., Yao, J., Huang, H., Chen, S., Liao, Z., Zhang, Q., Niyitanga, S., Yu, J., Liu, Y., Xu, X., Wang, J., Tao, A., Xu, J., Chen, S., Yang, X., He, Q., Lin, L., Fang, P., Zhang, L., Ming, R., Qi, J., & Zhang, L. (2021). Reference genomes of the two cultivated jute species. *Plant Biotechnology Journal*. https://doi.org/10.1111/pbi.13652

Zhao, Q., Wang, H., Yin, Y., Xu, Y., Chen, F., & Dixon, R.A. (2010) Syringyl lignin biosynthesis is directly regulated by a secondary cell wall master switch. *Proc. Natl. Acad. Sci. U.S.A.* 107(32), 14496–14501. https://doi.org/10.1073/pnas.1009170107

Zhou, J., Lee, C.,Zhong, R., & Ye, Z.H. (2009). *MYB58* and *MYB63* are transcriptional activators of the lignin biosynthetic pathway during secondary cell wall formation in Arabidopsis. *The Plant Cell*, 21, 248–266. https://doi.org/10.1105/tpc.108.063321

SUPPLEMENTARY FIGURE 1: Prediction of transmembrane helices in CcaLACs.

SUPPLEMENTARY FIGURE 2: Cis-acting elements in the upstream regions of CcaLACs.

SUPPLEMENTARY FIGURE 3: Validation of *in-silico* heatmap (transcriptomics) data using qRT-PCR.

SUPPLEMENTARY FIGURE 4: Comparative study of laccase (*CcaLAC*) gene expression in white jute cultivar JRC212 and its mutant line dlpf. This figure presents a comparative expression analysis of laccase (*CcaLAC*) genes in JRC212 and *dlpf* (which has fibres with 50% lower lignin content) across different developmental stages (30 DAS to 120 DAS).

SUPPLEMENTARY FIGURE 5: MicroRNA target prediction in *CcaLAC*s

SUPPLEMENTARY FIGURE 6: Gene Ontology (GO) term classification of the *CcaLAC* gene family.

SUPPLEMENTARY TABLE 1: List of primers

SUPPLEMENTARY TABLE 2: List of orthologous and paralogous pairs of *CcaLAC* genes

SUPPLEMENTARY TABLE 3: Protein features and chromosomal details of identified 34 *CcaLAC*s members in *Corchorus capsularis*

SUPPLEMENTARY TABLE 4: Functions of identified cis-regulatory elements in *CcaLAC* genes

SUPPLEMENTARY TABLE 5: miRNA Targets in *CcaLAC*s